ELSEVIER

Journal of Power Sources 72 (1998) 118–125

JOURNAL OF POWER SOURCES

An electrochemical impedance spectroscopy method for prediction of the state of charge of a nickel-metal hydride battery at open circuit and during discharge

Kenneth Bundy [a], Mikael Karlsson [a], Göran Lindbergh [b,*], Anton Lundqvist [b,1]

[a] *Chemical Technology, Department of Chemical Engineering and Technology, Royal Institute of Technology, KTH, SE-100 44 Stockholm, Sweden*
[b] *Applied Electrochemistry, Department of Chemical Engineering and Technology, Royal Institute of Technology, KTH, SE-100 44 Stockholm, Sweden*

Received 28 February 1997; revised 24 June 1997

Abstract

A multivariate method for predicting state of charge, from electrochemical data, of a nickel-metal hydride (NiMH)-battery is presented. Partial least square (PLS) regression is used to evaluate electrochemical impedance spectra and predict state of charge. The impedance spectra are analysed in the frequency range 239–0.6 Hz. The impedance is measured for different states of charge at open-circuit conditions and during continuous discharge at loads ranging between 0.2 C and 0.8 C. When measuring the impedance during discharge, the AC-current signal is imposed on the DC-current. The predictive capability of the method is tested by a cross validation procedure and the root mean square error of prediction is 7% when using the outlier identification capability of the PLS-regression method. The state of charge is evaluated with a single model, independently of whether the cell is subjected to open-circuit or polarised conditions. The predictive performance of the present model decreases at state of charge values less than 10%.

Keywords: Electrochemical impedance spectroscopy; NiMH battery; PLS-regression; State of charge

1. Introduction

Steady-state polarisation measurements are generally used for the determination of the performance and for the evaluation of kinetic parameters from battery electrodes. However, considerably more information is available from a study of the dynamic responses of such systems. In Electrochemical Impedance Spectroscopy (EIS) a small sinusoidal signal is used to perturb the electrochemical system and the response of the system is observed. The frequency of the signal is varied over a wide range, which makes it possible to monitor processes in the system with different time constants. EIS is a standard technique for investigation of electrochemical systems. However, it has been utilised to a smaller extent for analysis of the kinetics of porous electrodes. This is probably due to the greater difficulty in analysing the experimental results from these electrodes. The experimental results from simple electrode geometry can often be interpreted in the form of 'equivalent circuits'. This is a less suitable technique for the analysis of experimental results from porous battery electrodes, since it is difficult to describe the total impedance of a porous electrode with a simple 'equivalent circuit' or even with an analytical expression. The complexity of the problem has often led to the use of either lumped models which neglects the distribution of the reaction and the double layer charging in the porous structure, or simplified models which only accounts for some of the phenomena in the porous electrode.

Electrochemical techniques for the in situ evaluation of the state of charge (SoC) is of great practical importance for example during the utilisation of batteries for traction applications. A number of different methods for determining SoC, developed to match a particular battery system, have been suggested. As a general tool, EIS has been proposed. Most of the work done so far has been directed to find a linear dependence between some parameters, determined by EIS-measurement, and SoC. This parameter may be the impedance or a component in an equivalent circuit fitted to the experimental data. The major part of

* Corresponding author. E-mail: goeran.lindbergh@ket.kth.se
[1] Also corresponding author. E-mail: anton.lundqvist@ket.kth.se

the investigations have been performed under equilibrium condition, i.e., no load applied during measurement.

One early attempt to use EIS was determination of SoC for Zinc–Mercury Oxide primary cells [1]. In this case, both current–voltage characteristics and EIS were used with some success, finding a linear relationship for some of the parameters investigated. Okazaki et al. [2] used the second order harmonic of the impedance, at a single frequency, determining SoC for a lead–acid battery with an error less than 15%. So far, little work has been done to find a suitable way of determining SoC in the NiMH-battery. Qualitative studies of the change of impedance as a function of SoC and ageing was conducted by Reid [3,4]. However, no attempt was made to evaluate the possibility of using EIS as a state-of-charge indicator. The ageing effect upon the NiMH battery has also been studied by Smith et al. [5]. The need for determination of SoC, with an applied load was recognised by Blanchard [6]. A Ni–Cd battery was investigated at open circuit conditions and at constant discharge loads in the range 0–1 C. The impedance modulus was measured at a single frequency.

Equivalent circuits have also frequently been used. Reid studied the change in different parameters of a fitted equivalent circuit, for a Ni–Cd battery, as a function of SoC and cycle life [7]. It was however, difficult to draw any conclusions as for the possibility to use EIS for prediction of state of charge. Viswanathan et al. studied the impedance components of a Ni–Cd [8] and a lead–acid battery [9]. They also fitted the impedance data to a modified Randels' circuit. They found some of the impedance components monotonically increasing or decreasing as a function of SoC. For the Ni–Cd battery these components where found in the low frequency range. Sathyanarayana et al. [10] concluded that only a restricted number of impedance parameters, in the low frequency region, varied in a way useful for determination of SoC in a Ni–Cd battery.

As an alternative to EIS methods other perturbation signals have been used. Andrieu and Poignant [11] developed a fast method for determination of SoC. Instead of a sinusoidal signal, they used a pulse technique to determine the admittance, the inverse of the impedance. With this method, they could determine SoC for a single cell with an accuracy better than 15% over the entire range of SoC. Ilangovan and Sathyanarayana [12] proposed a galvanostatic alternative to the EIS procedure. The cell were discharged at a very low load for a few tens of seconds, and the voltage response was studied. It was possible to determine the parameters of an equivalent circuit from the voltage transient. These parameters were determined for a lead–acid battery though not as a function of SoC. Xiong et al. [13] used a similar method with a new procedure for calculation to simplify the evaluation. The method was applied to a Ni–Cd battery and was claimed to be superior at equilibrium conditions compared to an EIS-method. The evaluation of SoC for batteries under load was also studied but it was claimed that the complexity of the analysis restricted many of the used methods to laboratory research.

The problems, so far encountered, have been to find a usable parameter for determining SoC and a versatile method applicable at varying conditions, e.g., at an applied load. In this work, a multivariate approach, partial least square (PLS) regression, is proposed. The method is not restricted to the finding of a single parameter but uses a set of parameters built up internally in the PLS-regression model. The PLS-regression method has previously been used with success in interpreting the result from optical spectroscopy, e.g., for determination of nitrate in municipal waste water by UV-spectroscopy [14] and characterisation of chemical and physical descriptors of pulp using near-infrared spectrometry [15]. Multivariate methods have also been used for other purposes, in the context of battery research, e.g., for life-time and performance prediction of both Ni–Cd [16] and the lead–acid battery [17–19]. A PLS-pattern recognition method has also been used in the design of new metal-hydrides for use in the NiMH batteries [20].

PLS-regression is a method used to construct predictive models that relate some independent measurement, **X**, to a known response, **Y**. In this case, **X** represents the impedance data and **Y** represents state of charge values. Both the matrices **X** and **Y** can easily be extended, for example temperature and potential could be included in **X**. The method does not require a priori knowledge of the investigated system, but generates a model based entirely on the received data. Thus, the model is only valid within the experimental domain for which it was constructed. Using the model to predict data outside the experimental domain of reference measurements, i.e., extrapolation, is uncertain and should be avoided. The model gives no chemical information about the system, yet it is possible to use multivariate methods to achieve chemical information. This is a much more complicated process and requires more fundamental knowledge about the system.

The objective function of the method is to maximise the covariance between **X** and **Y**. This is done by utilising a new set of variables, the so-called PLS components. Information from all the original variables is projected down to a lower dimensional orthogonal space made up of the PLS components. A linear combination of these components makes up the model. The coordinates of the objects (one impedance spectrum is one object), in the space defined by the model, are called scores. Studying the score values can reveal trends and groups among the objects. The relationship between the original variables (single frequencies) and PLS components is captured by the loadings. A high loading value for an original variable means that this variable has a strong influence on that particular dimension of the model. The determination of the number of PLS components to be used in the model is a crucial step. Using to few components will leave out relevant information, while using too many will incorporate noise in the

model. Both these cases will impair the predictive capability of the model. The PLS regression method is extensively described in the literature, for instance by Martens and Næs [21] or Geladi and Kowalski [22].

2. Experimental

The measurements were run on a standard NiMH-cell with a nominal capacity of 2400 mAh (Varta VH2100). A nickel sheet was spot-welded to each of the terminals and two contacts were in turn soldered to the two nickel sheets. A Solartron 1287 electrochemical interface was used as galvanostat during all the experiments and was coupled to a Solartron 1255 Frequency Response Analyser for electrochemical impedance measurements. The instrument was controlled by the Corrware®- and ZplotW®-software on a PC. The cell was activated by cycling at 0.2 C, based on the nominal capacity, before the experiments. The cell was charged for 5 h and discharged to a cell voltage of 0.9 V. Impedance spectra were sampled at different states of charge, both at open circuit and at different discharge loads in the range of 0.2 C and 0.8 C. The discharge load was then held constant during each experiment. Between all experiments the cell was cycled once at 0.2 C to return it to its initial state. The impedance measurements were performed in galvanostatic mode and an alternating current signal with an amplitude of 100 mA was used. The frequency ranged between 600 Hz and 60 mHz, with five steps per decade. In the data analysis, a narrower range was used (see Section 3.1).

Open circuit experiments were conducted in the following way. The cell was charged with 0.2 C for 5 h and allowed to rest for 2 h. Impedance measurements were run at different SoC, stepped with approximately 10%, using a discharge load of 0.2 C, until the cell voltage reached 0.9 V. Before each impedance measurement, the cell was allowed to rest for 2 h. At the experiments during discharge, the cell was charged in the same way as for the OCP measurement. It was then discharged at constant load until it reached the SoC in question where the AC-signal was imposed on the DC discharge load, and an impedance measurement was conducted. The impedance was measured with steps of 10% in SoC at loads less than 0.4 C and with steps of 20% at loads greater than 0.4 C.

3. Treatment of data

3.1. Initial treatment of raw data

The impedance gets increasingly more scattered at low frequencies when the current is high. This comes about because the actual change of SoC during a measurement becomes important and because the analysis time on each frequency is short. At 0.8 C, the total change in SoC is 4.7% during an impedance measurement, whereas the change at 0.2 C is only 1.3%. The change in SoC, during a measurement, becomes more pronounced the lower the frequencies used. The applicability of the impedance method for fast evaluations is also impaired when using such time consuming, low frequencies. For these two reasons, the low frequency limit of data analysed, was set to 0.6 Hz. At the highest frequencies, impedance spectra showed an inductive behaviour which is believed to be caused by limitations in the experimental equipment. The upper limit of frequency was therefore set to 239 Hz. In some of the impedance spectra, one could also see some rejected data at some frequencies. This is not suitable when PLS regression is used for the analysis. Most of the missing values were due to failing of auto-integration, of the impedance, done by the FRA-unit. Some of the impedance values, returned by the FRA-unit, were still reasonable but it was decided that none of those were to be used. Instead, if no more than two subsequent values were missing, values were estimated using linear interpolation. If there were more than two subsequent values missing, the whole object (impedance spectrum) was omitted. The SoC at each impedance measurement was determined after each experiment, calculated from the total time of discharge at each discharge rate. It was chosen as the SoC when the sampling of the impedance was started. The omission of the low frequencies, reduced the change in SoC during one measurement to 1–2% at the highest discharge rates.

3.2. Treatment of data for PLS analysis

The experimental impedance data has been represented as complex numbers with a real and an imaginary part. Further analysis also showed that the influence on the PLS regression model was not equal for the real and imaginary part. The PLS regression method renders a large amount of freedom in preparing data for analysis. The predictive performance was enhanced by centring the data. The data was centred at each frequency by subtracting the average impedance at that frequency from the corresponding impedance values. In construction of the model it is also advantageous to try to avoid non-linearities in the dependence of the response, **Y**, on the independent variable, **X**. This can be achieved by pretreating **X** or **Y** with some suitable function. A number of functions were tried; f_i^2, $1/f_i$, $1/\sqrt{f_i}$, $1/(f_i^2)$, e^{f_i}, $\ln(f_i)$. These where used for modification of both the impedance data and the SoC values. None of these functions improved the performance of the model.

4. Results and discussion

4.1. General behaviour of the cell

The discharge behaviour at different discharge rates is shown in Fig. 1. From the discharge at 0.2 C, the total capacity was determined to 2200 mAh. While following all the reconditioning cycles, during the series of experiments,

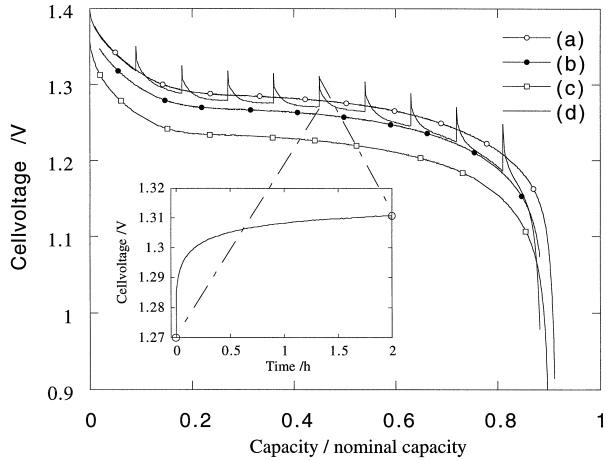

Fig. 1. The potential change of the cell at different discharge loads. Curves: (a) 0.2 C, (b) 0.4 C, (c) 0.8 C (d) open-circuit experiment. Included in the picture is also an example of the potential relaxation preceding measurement at open-circuit.

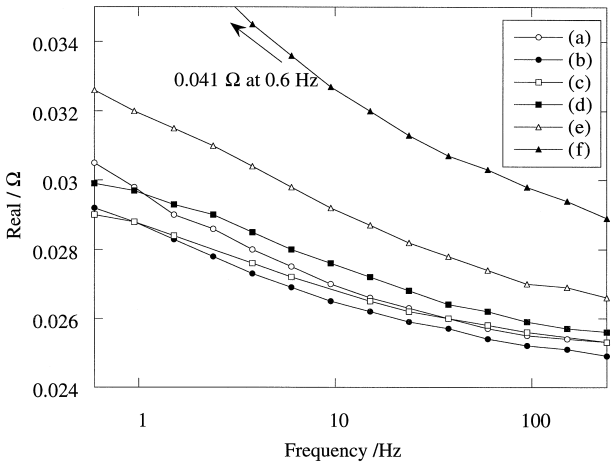

Fig. 3. The real part of the impedance, measured during discharge at 0.2 C, for different state of charge. The frequency range is 239–0.6 Hz. Curves: (a) 100%, (b) 77.9%, (c) 55.9%, (d) 33.6%, (e) 11.0%, (f) 0%.

the total capacity increased less than 2%. The discrepancy between the determined value and the nominal capacity arises partly from a reduced charging efficiency at the end of the charging. The charge supplied was 2400 mAh. Potential change at discharge during an 'open circuit measurement' is also shown in Fig. 1. An example of the potential change at open circuit, preceding the impedance measurement, is blown-up in Fig. 1. The determined capacity for an uninterrupted discharge at 0.2 C, and for the discharge during an OCP-measurement, differs about 3%, and can be attributed to random differences and, to some extent, to self-discharge. The OCP experiment, which includes the open circuit periods preceding each impedance measurement, takes about 24 h to complete. This is as opposed to an ordinary uninterrupted discharge completed in less than 5 h.

4.2. Impedance dependence upon SoC and discharge load

Figs. 2–5 are shown in the frequency range 239–0.6 Hz. Fig. 2 shows the impedance response for different SoC's from an experiment at a constant discharge load of 0.2 C, in a complex plane plot. Evidently, there are differences depending on the SoC. This dependence becomes even more evident, when looking only at the real part of the impedance, as seen in Fig. 3. The real part is seen to decrease, with increasing SoC, except at 100%, where the impedance is somewhat increased again. As the SoC approaches 0%, the real part is markedly increased especially at low frequencies. The dependence of impedance on discharge load is shown in Figs. 4 and 5, respectively, in the complex plane and as real part vs. frequency. The spectra were collected at SoC's ranging between 87.2 and 90.1%. There are significant differences seen, depending on the load, but no clear-cut relationship. It is interesting to see that the variations in the real part of the impedance, for different loads at 90% SoC (Fig. 5) is as big as the variations between 30–100% SoC at a constant load of 0.2 C (Fig. 3). This fact implies that a statistical method would be beneficial when predicting SoC at different discharge loads.

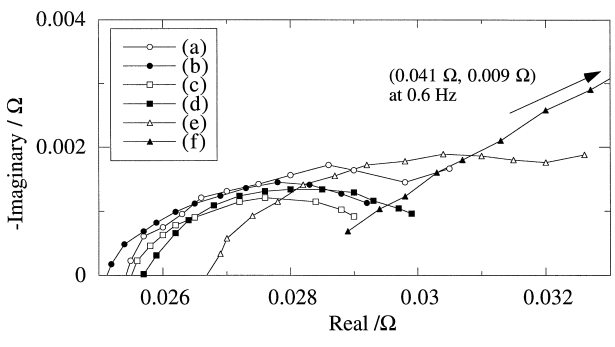

Fig. 2. Complex plane plot of the impedance, measured during discharge at 0.2 C, for different state of charge. The frequency range is 239–0.6 Hz. Curves: (a) 100%, (b) 77.9%, (c) 55.9%, (d) 33.6%, (e) 11.0%, (f) 0%.

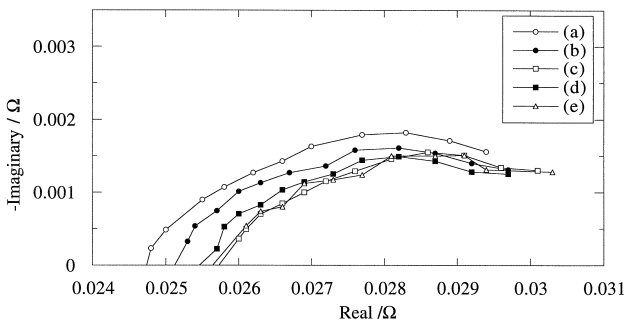

Fig. 4. Complex plane plot of the impedance, measured at open circuit (OCP) and at different discharge loads. The state of charge is approximately 90% and the frequency range is 239–0.6 Hz. Curves: (a) ocp, (b) 0.2 C, (c) 0.3 C. (d) 0.4 C, (e) 0.8 C.

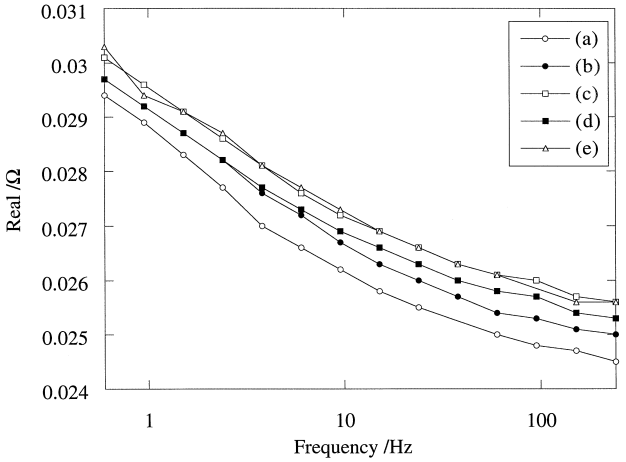

Fig. 5. The real part of the impedance, measured at open circuit (OCP) and at different discharge loads. The state of charge is approximately 90% and the frequency range is 239–0.6 Hz. Curves: (a) ocp, (b) 0.2 C, (c) 0.3 C. (d) 0.4 C, (e) 0.8 C.

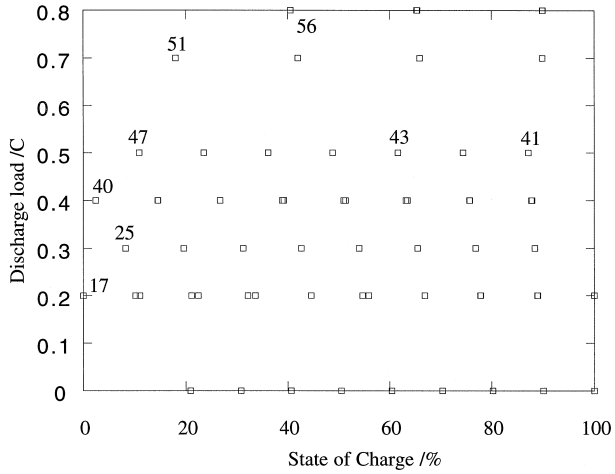

Fig. 6. The experimental domain used for construction of the PLS-regression model. Each point corresponds to one impedance measurement.

4.3. Multivariate analysis

To start with, it is to be emphasised that in the following predictions of SoC no information about cell voltage or discharge load has been used in constructing the multivariate model. In many cases knowledge of current load and potential for a constant current discharge, especially at laboratory conditions, would by itself be information enough to determine SoC. However in reality, this approach is difficult to adapt due to the flatness of the discharge curve (Fig. 1), and to the fact that the potential is not only dependent on SoC, but also on the previous history. Since the object of this work was to test the multivariate method on electrochemical impedance data, the only used information is the impedance spectra. If a discharge with fluctuating load was to be employed, e.g., for simulating electric vehicles, information about cell potential probably would improve the prediction of SoC. The experimental domain providing the basis of the PLS model is shown in Fig. 6.

The success of the PLS regression method depends on its ability to predict the SoC from an impedance spectrum. This ability is tested by a so-called cross-prediction procedure in the following way. A single object is removed and SoC, corresponding to that object, is predicted using a model constructed by the remaining objects. The object is removed to ensure that the predicted value itself does not influence the prediction. This procedure is then repeated for each of the objects in the experimental domain. The result from the cross-prediction is compiled in Fig. 7. The root mean square error, RMSEP, between measured and predicted values shows that the model predicts the SoC of the cell, independent of SoC and discharge load, with an average error of 11%. The solid line is a 45 degree line, which is the ideal result (the predicted value equalling the measured), and the dashed line is the linear regression line fitted to the cross-predicted data with a correlation coefficient of 0.85.

In Fig. 7, one can also see some values obviously less accurately predicted than the others. This is especially so for nos. 17 and 40 where each number corresponds to one point shown in the experimental domain (Fig. 6). A poorly predicted value could indicate that the underlying dataset in one way or another is different from the others. If this is the case the dataset is a so-called outlier. A good way to determine whether or not an object really is an outlier is a scoreplot (Fig. 8). In a scoreplot the score of each object

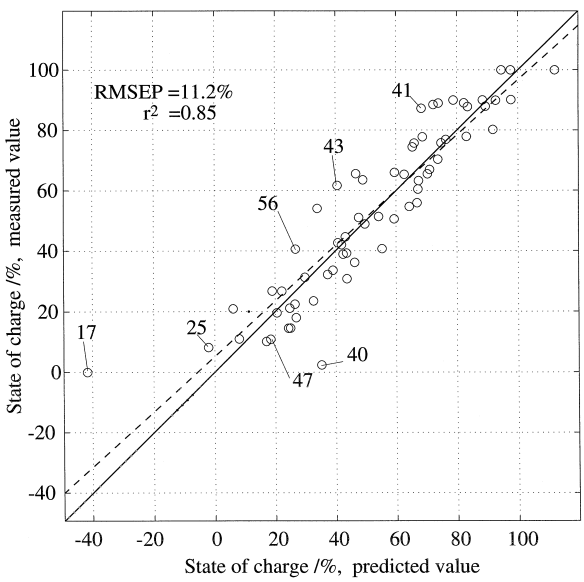

Fig. 7. Cross-prediction for state of charge without any outliers removed from the data. The dashed line is the linear regression line fitted to the cross-predicted data, with a correlation coefficient r^2 of 0.85. The root–mean square error between the predicted and measured values is 11.2%. Numbers indicated in the figure correspond to those indicated in Fig. 6.

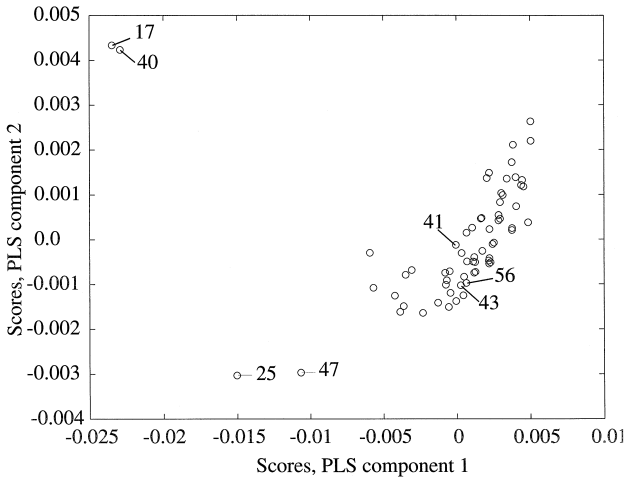

Fig. 8. The scoresplot for PLS-component 2 vs. PLS-component 1. Numbers indicated in the figure correspond to those indicated in Fig. 6.

for the different PLS-components are plotted against each other. In Fig. 8, the scores of the first PLS-component are plotted against the scores of the second. The scores reflect the inherent properties of the model and contain information about both impedance and SoC. As seen in Fig. 8, all the data are collected together, except nos. 17, 25, 40 and 47. All these are thus considered as outliers by the model. Other similar plots also indicated nos. 41, 43 and 56. Since the objective was to find a method that is easy to use, it was decided that all outliers, indicated by the model, were to be removed. Afterwards these outliers could be analysed to find plausible reasons for their behaviour. The result from the cross-prediction, with the seven outliers indicated

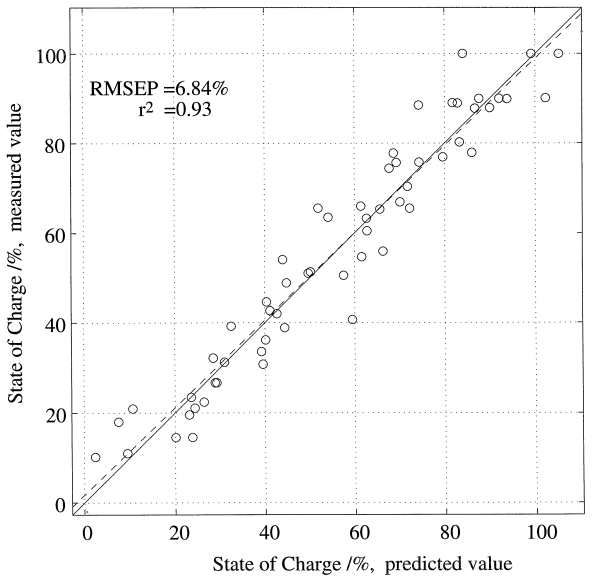

Fig. 9. Cross-prediction for state of charge with the seven outliers indicated by the analysis removed. The dashed line is the linear regression line fitted to the cross-predicted data, with a correlation coefficient r^2 of 0.93. The root–mean square error between the predicted and measured values is 6.8%. Numbers indicated in the figure correspond to those indicated in Fig. 6.

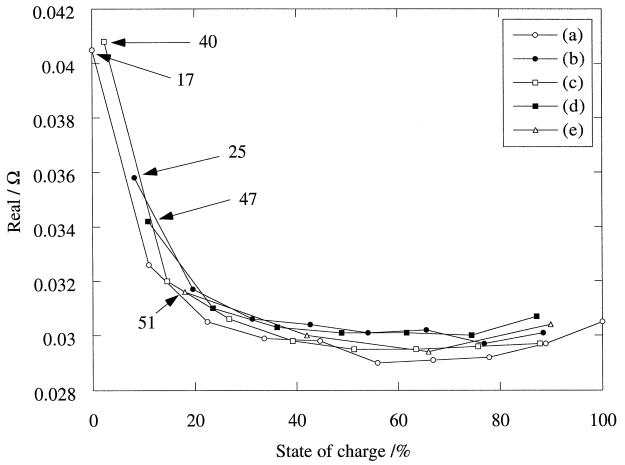

Fig. 10. The real part of the impedance, measured at 0.6 Hz, as a function of state of charge for different discharge loads. Four outliers are indicated (nos. 17, 25, 40, 47) in the picture together with a point not indicated as an outlier (no. 51). Numbers indicated in the figure corresponds to those indicated in Fig. 6. Curves: (a) 0.2 C, (b) 0.3 C, (c) 0.4 C, (d) 0.5 C, (e) 0.7 C.

by the model removed, is plotted in Fig. 9. The RMSEP value was then decreased to less than 7%.

When a satisfactory result was obtained, the focus was turned to the outliers. It was noted that four outliers, nos. 17, 25, 40 and 47, were all situated at the left edge of the experimental domain (Fig. 6), corresponding to low SoC. The real part of the impedance for the discharge loads corresponding to the above outliers, as a function of SoC, was studied. This comparison is plotted in Fig. 10 where each symbol represents a single point in the experimental domain. The different outliers are indicated in the figure. When looking at nos. 17, 25, 40 and 47, one sees that all of them undergo a marked change in impedance compared to the other points. The change in impedance in the last 10% of SoC is markedly larger, than the total variation in impedance for the former 90%. Since the model is constructed by linear combinations, it is no wonder that such a strong non-linear behaviour causes special problems. Point 51, also situated at the left edge of the experimental domain, does not show this sharp increase in impedance, and is not indicated as an outlier. The outliers 41, 43 and 56 could not be explained by a visual inspection. A conclusion from studying the outliers is that prediction problems, due to the non-linear behaviour in the end of the discharge, can be expected. The problem might be reduced by increasing the number of points in the non-linear area of the experimental domain. Another possibility is to use another model to determine SoC, e.g., lower than 10%. As previously noted, the pretreatment of the data had no obvious effect on this problem. It could be interesting to see how a model applicable between 10% to 100% SoC, would behave without any outliers removed. This case approximately corresponds to removal of the four outliers 17, 25, 40 and 47 only, and thus a third model was

constructed. The RMSEP of the prediction was reduced to 9%.

To further study the development of the model, the prediction residuals, i.e., the difference between the predicted and measured values, were studied. Residuals for the three models are plotted in Fig. 11. If the residuals are random, i.e., normally distributed around zero, one can assume that no more information can be extracted from the data. As seen in Fig. 11, the residuals for the model approach the normal distribution around zero as more outliers are removed. The residual distribution for the model with seven outliers removed led us to believe that this was a satisfactory model.

The PLS regression model is built up by a linear combination of PLS components. By plotting the so-called loadings for each PLS component, one can get a picture of the influence of each frequency for each PLS component. These loadings are plotted for PLS component 1, 2 and 6 in Fig. 12. The relative influence of each frequency is measured as the distance to the zero-level. One can see that the low frequency region of impedance has a stronger influence, although it can be seen for both PLS component 1 and PLS component 2, that the whole spectrum is used. Loadings for PLS component 6, which is the last component used, seems to be more randomly distributed among the frequencies. This is an indication that further addition of PLS components would only describe a randomised behaviour.

The aim of this work has been to present a new method showing how PLS-regression coupled to EIS can be used for prediction of SoC being aware that further work remains before practical use in, e.g., an electric vehicle. This investigation is done under laboratory conditions and a technical battery system will introduce a number of additional parameters such as age, prehistory and temperature and quite often the additional difficulty of a system consisting of a large number of cells. These factors will further increase the complexity of the analysis.

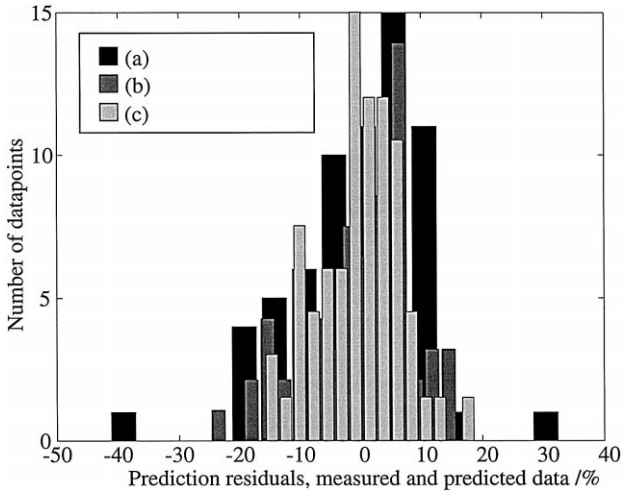

Fig. 11. The prediction residuals for three different models with different number of removed outliers. Curves: (a) no outliers removed, (b) 4 outliers removed, (c) 7 outliers removed.

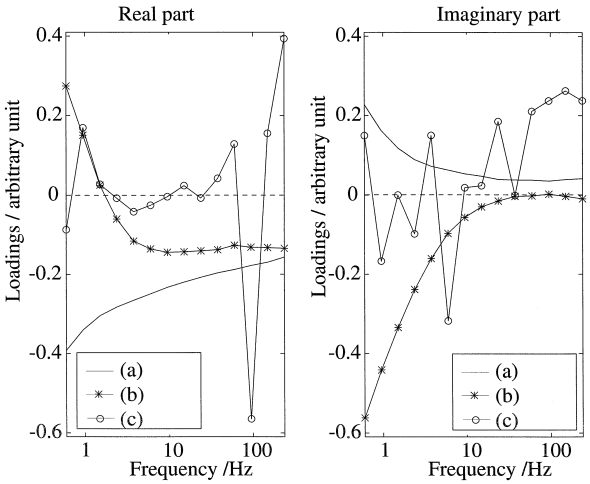

Fig. 12. The loadings for three PLS-components for the model without any outliers removed. Curves: (a) PLS component 1, (b) PLS component 2, (c) PLS component 6.

The presented method is believed to have certain advantages when considering the use in technical systems. The method does not require the construction of an equivalent circuit and is not directly impaired by the porous character of the electrodes. The fitting of data, to an equivalent circuit, before estimation of state of charge is not necessary. Instead the calculation becomes a matrix multiplication once the model parameters are determined. This is important since fitting procedures are often very tedious whilst matrix multiplication is fast. The problem of parameters such as cycle life and temperature may be handled by introducing them in the model and one can also use the cell voltage as a variable. This is done in a straightforward way using the presented method but may be a problem with other methods since it is not obvious how to include these parameters. Any number or type of perturbation signal can also be used in a model to increase the performance. The incorporation of new experimental data into the matrix of experimental data is easy which makes it possible to calibrate and update the system. The PLS-regression has also an outlier identification capability. Thereby, it is possible to determine whether or not a measurement is valid or not in perspective of the calibration data. The drawback of the PLS-regression method is that it does not give any specific chemical information about the battery and that predictions outside the experimental domain of reference measurement are difficult. This is handled by constructing a domain of calibration measurements that include the normal use of the battery.

5. Conclusions

A multivariate method for predicting state of charge, from electrochemical data, of a nickel-metal hydride

(NiMH)-battery is presented. The impedance was measured for different states of charge at open-circuit conditions and during continuous discharge. PLS-regression was used to evaluate the electrochemical impedance spectra and predict state of charge without a priori knowledge of the electrochemical system.

The predictive capability of the method was tested by a cross-validation procedure and the root mean square error of prediction was as low as 7% when using the outlier identification capability of the PLS-regression method.

The presented model works best in a range of state of charge between 10–100% both at open-circuit and during a constant current discharge.

Acknowledgements

The authors are grateful to Dr. Per Ekdunge, AB Volvo, for initiating this study. This work was partially financed by The Swedish Research Council for Engineering Sciences (TFR).

References

[1] J.J. Winter, J.T. Breslin, R.L. Ross, H.A. Leupold, F. Rothwarf, J. Electrochem. Soc. 122 (1975) 1434.
[2] S. Okazaki, S. Higuchi, S. Takahashi, J. Electrochem. Soc. 132 (1985) 1516.
[3] M. Reid, in: P.D. Bennett, T. Sakai (Eds.), Hydrogen and Metal Hydride Batteries/1994, PV 94-2, p. 237, The Electrochemical Society Proceedings Series, Pennington, NJ (1994).
[4] M. Reid, J. Power Sources 47 (1994) 277.
[5] R.L. Smith, A.V. Bray, D.K. Coates, IEEE 35th International Power Sources Symposium, Cherry Hill, NJ, June 1992, p. 156.
[6] Ph. Blanchard, J. Appl. Electrochem. 22 (1992) 1121.
[7] M. Reid, Electrochim. Acta 38 (1993) 2037.
[8] V.V. Viswanathan, A.J. Salkind, J.J. Kelly, J.B. Ockerman, J. Appl. Electrochem. 25 (1995) 716.
[9] V.V. Viswanathan, A.J. Salkind, J.J. Kelly, J.B. Ockerman, J. Appl. Electrochem. 25 (1995) 729.
[10] S. Sathyanarayana, S. Venugopalan, M.L. Gopikanth, J. Appl. Electrochem. 9 (1979) 125.
[11] X. Andrieu, P. Poignant, Power Sources 14 (1993) 43.
[12] S.A. Ilangovan, S. Sathyanarayana, J. Appl. Electrochem. 22 (1992) 456.
[13] X.Y. Xiong, H.V. Poorten, M. Crappe, Electrochim. Acta 41 (1996) 1267.
[14] M. Karlsson, B. Karlberg, R.J.O. Olsson, Anal. Chim. Acta 312 (1995) 107.
[15] R.J.O. Olsson, P. Tomani, M. Karlsson, T. Joseffson, K. Sjöberg, C. Björklund, Tappi J. 78 (1995) 158.
[16] W.A. Byers, S.P. Perone, J. Electrochem. Soc. 126 (1979) 720.
[17] S.P. Perone, R. Petesch, P. Chen, W.C. Spindler, S.L. Deshpandé, J. Power Sources 37 (1992) 379.
[18] S.P. Perone, J. Power Sources 13 (1984) 23.
[19] A.L. de Azevedo, F.B. Diniz, B.B. Neto, J. Power Sources 52 (1994) 87.
[20] H. Liu, J. Guo, N. Chen, T. Huang, Anal. Lett. 29 (1996) 341.
[21] H. Martens, T. Næs, Multivariate Calibration, Wiley, Chichester, 1991.
[22] P. Geladi, B.R. Kowalski, Anal. Chim. Acta 185 (1986) 1.